

FEM modelling for press bend forming of doubly curved integrally stiffened aircraft panel

YAN Yu¹, WANG Hai-bo¹, WAN Min²

1. College of Mechanical and Electrical Engineering, North China University of Technology, Beijing 100144, China

2. School of Mechanical Engineering and Automation, Beihang University, Beijing 100191, China

Received 9 July 2012; accepted 15 August 2012

Abstract: In order to establish an FEM model for aircraft integral panel press bend forming process, a special simulation procedure and a calculation method for the punch and die boundary condition based on the bending line coordinates were proposed. The simulation of a seven-step press bend forming process of doubly curved integrally stiffened aircraft panels was realized, and it could well simulate the real fabrication process, so that it could assist in studying this complicated forming process. Stress and strain distributions were analyzed, which reveals the deformation mechanics of this process. With quantitative comparisons, it can be concluded that forming quality of the seven step press bend forming is quite good, considering both the forming precision and the surface quality.

Key words: press bend forming; integrally stiffened aircraft panel; double curvature contour; FEM modelling

1 Introduction

Integrally stiffened panels are widely used today on advanced aircrafts because of their light weight and high stiffness. “Integrally stiffened” means skin and stringers are integrated into a single structure [1]. But because of the complexity of the structure, the high precision of the contour, and the requirements of good mechanical properties, fabrication of this kind of aircraft panel becomes a great challenge to the aircraft manufacturing industry. Research on the forming of long life and low cost aircraft wing panels and fuselage panels is urgently needed.

As a traditional and widely used forming method for integrally stiffened aircraft panels, press bend forming possesses some advantages, such as low tooling cost, short cycle time and adaptability to different contours [1]. But press bend forming is operator dependent and the process parameters should be chosen carefully to avoid buckling and fracture on stiffeners and to form the desired contour. Research on this process to improve the forming quality and efficiency is very important. Comparing with the theoretical analysis and experiment, numerical simulation is a method beyond

comparison for the advantages, obtaining plenty of historical information and considering the influence of multiple factors on the process [2]. Establishment of the reliable FE model is the key point for studying the complex forming process [3, 4]. There appears to be very little previous work in the literature on the press bend forming of aircraft panels. LIU et al [5–12] carried out some valuable and fundamental experimental and numerical studies on press bend forming to analyze the strain and stress distribution, the springback, and the self-adapting incremental press bending. But a lot of detailed work still needs to be done. First, both bending and springback were simulated with an explicit algorithm in their study. The principles of the explicit algorithm determine that the stress calculated with the explicit algorithm is not accurate enough, while the stress field of the forming stage decides the precision of the springback calculation. Although it is commonly accepted that using an explicit algorithm to analyze the forming stage and an implicit algorithm to analyze the springback stage is an efficient way of simulation, many researchers recommend calculating both forming and springback with an implicit algorithm [13]. YAN et al [14–17] established FEM model of press bend forming of simple curvature specimens, and proposed the FEM equivalent

model for this process in order to improve the calculation efficiency. They also established the fracture prediction model and buckling prediction model for the press bend forming process. But similarly, only the press bend forming of the simple curvature panel was modelled, while almost all the wing panels have double curvature contour. In fact, it is quite difficult to model the double curvature press bend forming process. The panel deforms freely in 3D space, so the movements of the edges are rather complicated, especially for bending when the bend lines are not perpendicular to the edges of the panels. Thus, it is hard to establish the boundary condition of the panel. In addition, the forming of compound contour panels is a multi-step process, and the simulation of the bending at different bend lines needs accurate repositioning of the deformed panel and dies. Therefore, FEM modelling involves calculation of the movements of the dies and complicated contact conditions. No similar FEM modelling has been found in the literature.

In this work, an introduction to the press bend forming process of doubly curved stiffened aircraft panels was given. And then a new FEM modelling method for the simulation of this bending technology was presented. A calculation algorithm of the boundary conditions of the punch and dies was proposed. The final strain and stress state will be calculated with the simulation result of a seven-step press bend forming of a doubly curved aircraft integral panel.

2 Description of press bend forming process

Based on the three point bending principle, press bend forming is a multi-step bending process with universal dies according to planned forming paths, as shown in Figs. 1 and 2. The equipment is a simple press

brake that is usually operated manually. When the bending at one location finishes, the panel is incremented to the next bend line and another bend performs. Finally, a series of overlapped bending form the simple or compound curvature contour of aircraft wing panels.

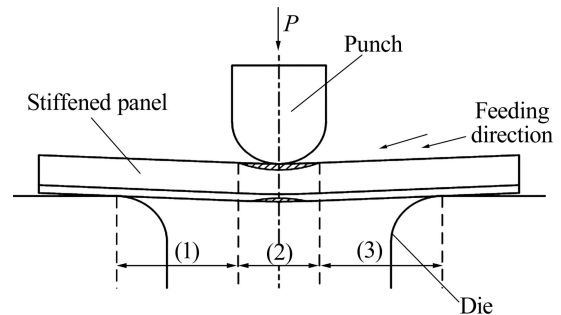


Fig. 1 Schematic illustration of press bend forming at one position: (1) Elastic deformation section; (2) Plastic deformation section; (3) Elastic deformation section

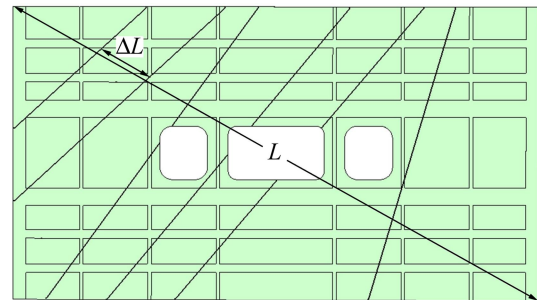


Fig. 2 Schematic illustration of press bend forming path

3 FEM modelling and simulation details

3.1 Geometry

As shown in Fig. 3, the specimen panel with typical stiffener cross sections is designed according to the

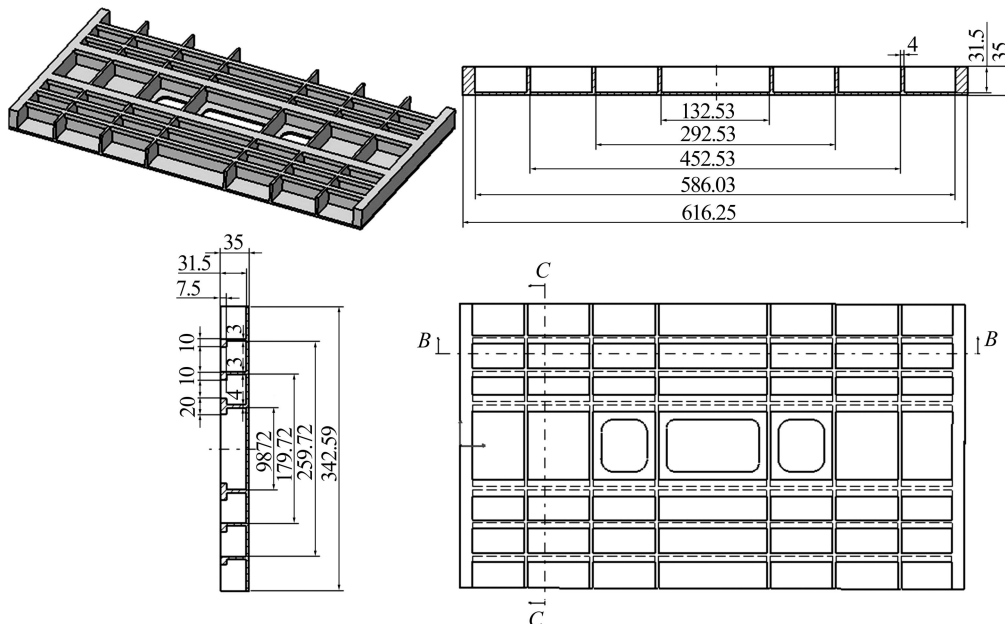


Fig. 3 Dimensions of designed specimen panel (Unit: mm)

structures of the real aircraft wing panels. In order to keep the comparability, the radius of the punch and die is taken to be 35 mm, which is the same as the real punch and die dimensions in the aircraft manufacturing factory. The die gap is 70 mm. The objective shape curvature of this integral panel is shown in Fig. 4. It is shown that the curvature distribution is not desultory. It decreases from the left to the right, so the left part is obviously curved and the right part is relatively flat.

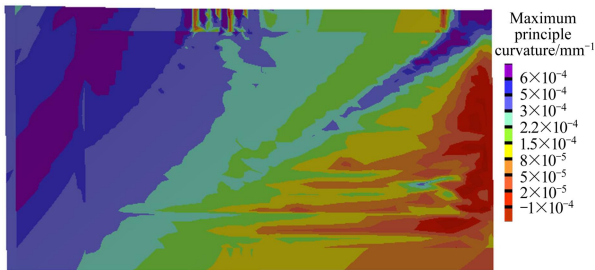


Fig. 4 Maximum principle curvature distribution of objective skin outer surface

3.2 Material properties

The material of the integrally stiffened panel is aluminium alloy 7B04-T7451, whose elastic modulus is 69 GPa, and initial yield stress is 447.51 MPa. The friction coefficient is assumed to be 0.1. Uniaxial tensile tests were carried out and the test data were entered into the FEM software ABAQUS. The uniaxial tensile test data are shown in Fig. 5. According to $|\sigma| = \sigma_s + K|\varepsilon^P|^n$ [18], the hardening exponent and the hardening coefficient that fitted with the test data are 0.91 and 1817.66, respectively.

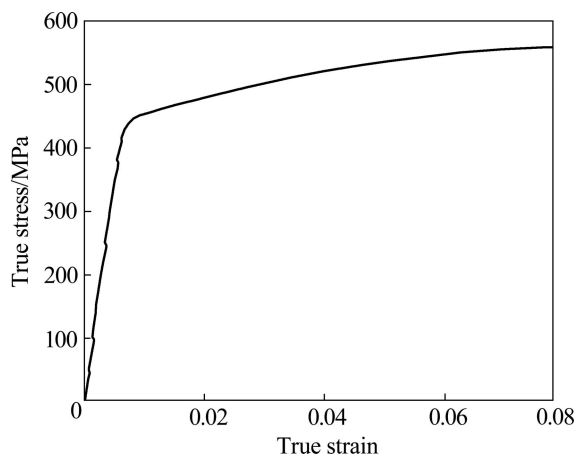


Fig. 5 Uniaxial tensile test result

3.3 Yield criterion

The model adopts the von Mises yield criterion, because the rolling direction of the material doesn't play an important role in this forming process.

3.4 Time integration scheme

Though the explicit integration method is more efficient than the implicit integration method, it is generally recognized that implicit integration method has a higher precision. Moreover, in order to avoid constantly transferring between the explicit and implicit algorithms for the multi-step press bend forming, both the forming and springback processes were simulated with ABAQUS/Standard. Complete tool removal including contact interactions was adopted to simulate the springback of the panel.

3.5 Contact algorithm

The penalty method and the Coulomb friction model were adopted. The penalty method approximates hard pressure-overclosure behaviour. With this method, the contact force is proportional to the penetration distance, so some degree of penetration will occur. The basic concept of the Coulomb friction model is to relate the maximum allowable frictional (shear) stress across an interface to the contact pressure between the contacting bodies.

3.6 Element type and meshing

Since second-order (quadratic) interpolation elements have difficulties in contact simulation, first-order, reduced-integration elements in ABAQUS including hourglass control were adopted. The panel was modelled mainly with 3D brick elements (C3D8R) and a few linear wedge elements (C3D6), and the punch and dies are modelled with rigid shell element (R3D4).

Because of the particularity of this forming process, tremendous amount of elements are needed. First, the dimension of the panel is very large in itself, while the stiffeners are tall and thin. In order to ensure the calculation precision, the number of the elements through the stiffener thickness direction should be more than two, which certainly lead to more elements. Second, the punch and die are quite small compared with the panel, so the outer surface of the panel skin can't be meshed too coarse, otherwise the penetration would be significant. And third, multi steps of bending at different positions make the local refining not invalid. The total number of the panel elements is 137848, which is so large and will certainly lead to long calculation time. Therefore, there isn't a good way to reduce the number of elements, and an equivalent model is essential.

3.7 Assembly of model

The press bend forming process is planned to bend orderly from the left hand side to the right hand side at seven bend lines. The origin point of the assembly is set

at the midpoint of the first bend line and the die length direction is along the first bend line, as shown in Fig. 6, in which the borders of different colours represent the bend lines. To avoid the divergence of the contact interaction calculations, the punch and dies are in contact with the panel's top and bottom surfaces with zero clearance. Because this may help ABAQUS/Standard examine the state of all contact interactions at the beginning of the simulation to establish whether slave nodes are open or closed, thus further iterations can be conducted more smoothly to achieve equilibrium.

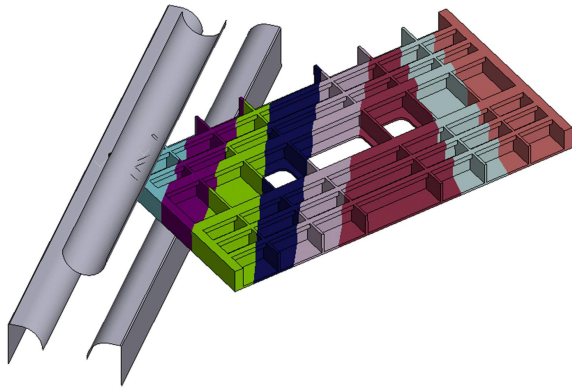


Fig. 6 FE assembly of press bend forming model

3.8 Simulation procedure and boundary condition

According to the press bend forming path that was designed based on the experiences in the aircraft factory, seven bending and springback steps were adopted. Some additional steps were used to reposition the deformed panel after a certain press bending operation, to move the punch and dies to the successive bend lines, and to build up the contact interaction.

Because the bend lines are not always perpendicular to the edges of the panel, the counter acting forces from the left and right die are not equal. Thus, the panel is prone to slip to one side when the punch lowers if no proper boundary condition is specified. But the movements of the edges or the vertexes of the panel can't be predicted, for the bending and springback are highly flexible 3D deformation processes. So constraining the movements of the edges or the vertexes of the panel is impracticable. Applying concentrated load or pressure load also falls short of the real forming process and couldn't control the forming appropriately. A solution to this problem was proposed, in which the cross section of the panel at the bend line was assumed to be the surface of symmetry. At the very beginning of bending process, the symmetric boundary condition along the surface of symmetry in the panel was retained by constraining the nodes on this surface, and the boundary conditions of each cross section of the bend

line were set according to the correspondent local coordinate system in FE software. To generate part mesh that contains nodes exactly at the surfaces of symmetry, the CAD panel model is partitioned in advance at the planned bend lines.

The simulation procedure and the correspondent boundary condition instructions are shown in Fig. 7.

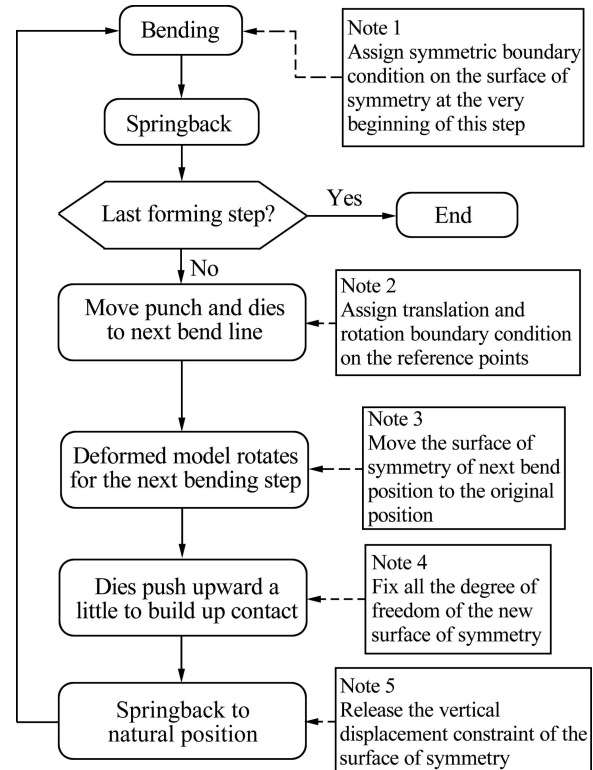


Fig. 7 Flow chart of simulation procedure and boundary conditions

3.9 Calculation of the motion of punch and dies

In the FEM modelling of the multi-step press bend forming, positioning of the machined panel in the successive forming steps was a complicated problem. Because the movements of the rigid bodies are easy to be controlled in the FE software, moving the punch and dies instead of the panel was adopted to realize the bending and springback at different positions. According to the determined press bend forming path, which is represented by the intercepts of the bend line on the panel edges, the translation and rotation of the punch and dies were calculated as the boundary conditions in the FEM model. With the comprehensive understanding of the initial working state and the process procedure, a strict deduction of the geometric relations was conducted. In order to make the calculation universal, an arbitrary quadrangle was adopted to represent the outline of the machined panel, as shown in Fig. 8. The algorithm of the program that calculates the movements of the punch and dies is as follows.

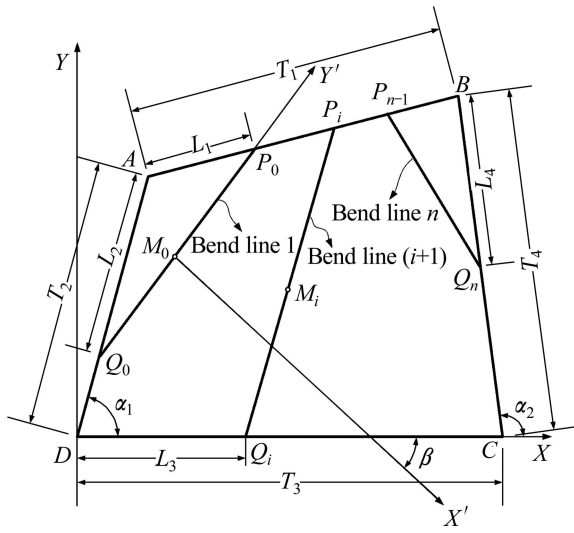


Fig. 8 Schematic illustration of bend line positions

- 1) Read in the number of the bend lines n .
- 2) Read in the lengths and the obliquities of the panel edges: $T_1, T_2, T_3, T_4, \alpha_1$ and α_2 . Then calculate the coordinates of the four vertexes of the panel.

Vertex A:

$$x_A = T_2 \cos \alpha_1 \quad (1)$$

$$y_A = T_2 \sin \alpha_1 \quad (2)$$

Vertex B:

$$x_B = T_3 + T_4 \cos \alpha_2 \quad (3)$$

$$y_B = T_4 \sin \alpha_2 \quad (4)$$

Vertex C:

$$x_C = T_3 \quad (5)$$

$$y_C = 0 \quad (6)$$

Vertex D:

$$x_D = 0 \quad (7)$$

$$y_D = 0 \quad (8)$$

- 3) Read in the intercepts of the first bend line on the panel edges: $L_1[0], L_2[0], L_3[0]$, and $L_4[0]$. Then calculate the coordinates of the endpoints P_0, Q_0 and the midpoint M_0 of the first bend line.

$$x_P[0] = \frac{L_1[0]}{T_1} \cdot (x_B - x_A) + x_A \quad (9)$$

$$y_P[0] = \frac{L_1[0]}{T_1} \cdot (y_B - y_A) + y_A \quad (10)$$

If Q_0 is on line AD, then

$$x_Q[0] = (T_2 - L_2[0]) \cdot \cos \alpha_1 \quad (11)$$

$$y_Q[0] = (T_2 - L_2[0]) \cdot \sin \alpha_1 \quad (12)$$

Else if Q_0 is on line CD, then

$$x_Q[0] = L_3[0] \quad (13)$$

$$y_Q[0] = 0 \quad (14)$$

Else Q_0 is on line BC, then

$$x_Q[0] = (T_4 - L_4[0]) \cdot \cos \alpha_2 + T_3 \quad (15)$$

$$y_Q[0] = (T_4 - L_4[0]) \cdot \sin \alpha_2 \quad (16)$$

The coordinates of the midpoint M_0 is

$$x_M[0] = \frac{x_P[0] + x_Q[0]}{2} \quad (17)$$

$$y_M[0] = \frac{y_P[0] + y_Q[0]}{2} \quad (18)$$

- 4) Build up the local coordinate system $X'M_0Y'$, of which the origin point is coincident with the midpoint M_0 and the Y' axis is coincident with the first bend line, as shown in Fig. 8.

- 5) Read in the intercepts of the $(i+1)$ th bend line on the panel edges: $L_1[i], L_2[i], L_3[i]$, and $L_4[i]$. Then calculate the coordinates of the endpoints P_i and Q_i .

$$x_P[i] = \frac{L_1[i]}{T_1} \cdot (x_B - x_A) + x_A \quad (19)$$

$$y_P[i] = \frac{L_1[i]}{T_1} \cdot (y_B - y_A) + y_A \quad (20)$$

If Q_i is on line AD,

$$x_Q[i] = (T_2 - L_2[i]) \cdot \cos \alpha_1 \quad (21)$$

$$y_Q[i] = (T_2 - L_2[i]) \cdot \sin \alpha_1 \quad (22)$$

Else if Q_i is on line CD,

$$x_Q[i] = L_3[i] \quad (23)$$

$$y_Q[i] = 0 \quad (24)$$

Else Q_i is on line BC,

$$x_Q[i] = (T_4 - L_4[i]) \cdot \cos \alpha_2 + T_3 \quad (25)$$

$$y_Q[i] = (T_4 - L_4[i]) \cdot \sin \alpha_2 \quad (26)$$

- 6) Calculate the horizontal displacements of the punch and dies.

In ABAQUS/Standard, the boundary condition is defined by the absolute coordinate, so the displacements

of the punch and die in any moving step should be calculated according to the original assembly position. Because the origin point of the assembly is coincident with the midpoint of the first bend line M_0 , and the die length direction is along the first bend line direction, as shown in Fig. 8, the coordinates of the midpoint of the $(i+1)$ th bend line M_i after coordinate transformation can be taken as the horizontal displacements of the punch and dies.

The coordinates of the midpoint of the $(i+1)$ th bend line M_i in the original coordinate system are

$$x_M[i] = \frac{x_P[i] + x_Q[i]}{2} \quad (27)$$

$$y_M[i] = \frac{y_P[i] + y_Q[i]}{2} \quad (28)$$

Transform these coordinates to $X'M_0Y'$. After displacement transformation,

$$x_M[i]' = x_M[i] - x_M[0] \quad (29)$$

$$y_M[i]' = y_M[i] - y_M[0] \quad (30)$$

After rotation transformation,

$$x_M[i]'' = x_M[i]' \cdot \cos \beta + y_M[i]' \cdot \sin \beta \quad (31)$$

$$y_M[i]'' = y_M[i]' \cdot \cos \beta - x_M[i]' \cdot \sin \beta \quad (32)$$

7) Calculate the rotation angle of the punch and dies according to the original coordinate system, for the rotation angle is independent of the coordinate system and it is much easier to calculate with the original coordinates instead of the transformed coordinates. The slope of the first bend line is

$$k_0 = \frac{y_Q[0] - y_P[0]}{x_Q[0] - x_P[0]} \quad (33)$$

If $x_p[i] = x_q[i]$, the $(i+1)$ th bend line is vertical according to the original coordinate system, then the rotation angle of the $(i+1)$ th punch and die is

$$\gamma = \frac{\pi}{2} - \arctan(k_0) \quad (34)$$

Else, calculate the slope of the $(i+1)$ th bend line:

$$k_i = \frac{y_Q[i] - y_P[i]}{x_Q[i] - x_P[i]} \quad (35)$$

If $k_0 = -\frac{1}{k_i}$, the two lines are orthogonal, then

$$\gamma = \pm \frac{\pi}{2} \quad (36)$$

Else,

$$\gamma = \pm \arctan\left(\frac{k_i - k_0}{1 + k_i \cdot k_0}\right) \quad (37)$$

8) Output the horizontal displacements: $x_M[i]''$, $y_M[i]''$, and the rotation angle of the $(i+1)$ th punch and die γ .

9) Repeat the calculations from step 5) to step 8) for $(n-1)$ times.

10) The end.

4 Results and discussion

4.1 Mises stress distribution

The punch strokes at seven bend lines from left to right are 0.2, 3.3, 3.1, 2.9, 2.8, 2.7 and 2.5 mm. The Mises stress distributions at the end of each bending step are shown in Fig. 9. At the beginning of the forming process, the bending of each position affects only a small part of the panel, and the residual stress exists at the vicinity of the bending lines. And compared with the outer surface of the skin, the normal bending stress of the stiffener top is larger, as it is farther from the neutral surface. With the proceeding of the forming, because the bending positions of press bend forming are too close to each other, the influences among different bending steps could be so remarkable that the deformation areas may overlap each other. Therefore, the panels experience cyclic loading and unloading conditions or other remarkable changes of the stress conditions. Stiffeners play an important role in passing the punch force to the whole panel and they are apt to buckle with the lowering of the punch, so the process parameters need to be chosen elaborately to form the objective contour without the occurrence of the buckling and fracture on stiffeners.

4.2 Plastic strain distribution

The equivalent plastic strain distribution of the model is shown in Fig. 10. It can be seen that the plastic strain mainly distributes at the bending lines. In addition, the surface of the stiffened panel is smooth with no buckling on the stiffeners. Therefore, not only the shape accuracy but also the surface quality is ensured.

4.3 Final outer skin surface

To examine the forming precision, and extract the outer skin surface of the formed part, the contrasts of the formed panel outer surfaces with the discrete objective shape surface are shown in Fig. 11. It can be seen that the forming error is quite small.

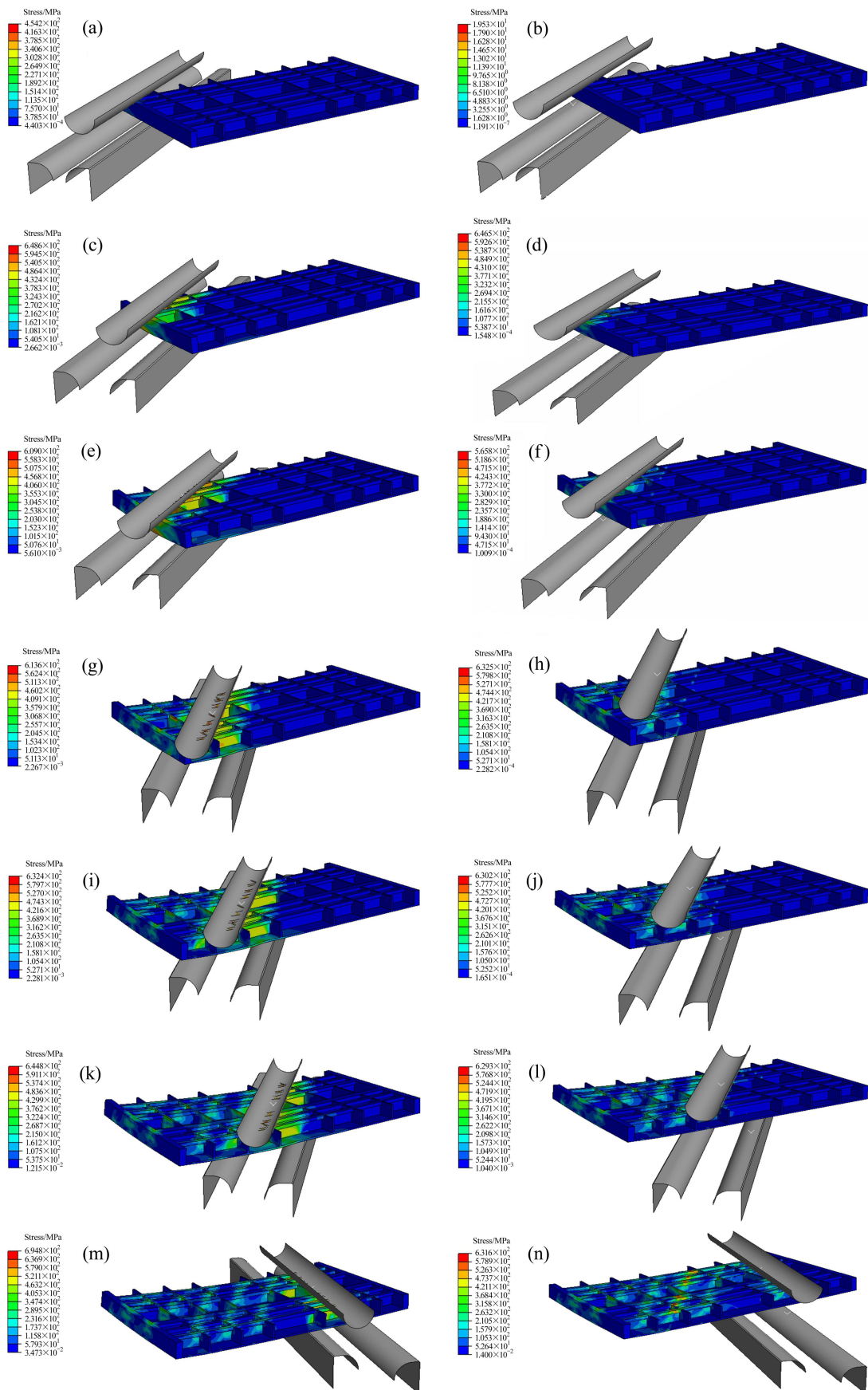


Fig. 9 Mises stress distribution during forming process: (a) Bending 1; (b) Springback 1; (c) Bending 2; (d) Springback 2; (e) Bending 3; (f) Springback 3; (g) Bending 4; (h) Springback 4; (i) Bending 5; (j) Springback 5; (k) Bending 6; (l) Springback 6; (m) Bending 7; (n) Springback 7

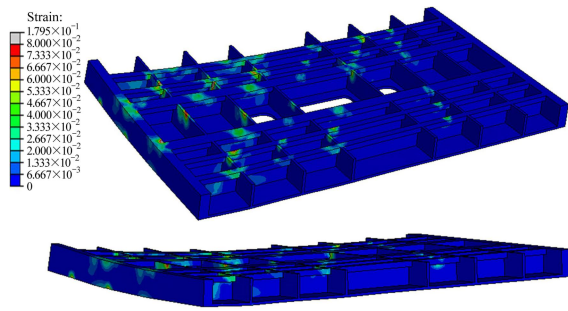


Fig. 10 Equivalent plastic strain distribution of formed panel

- Objective shape
- Outer skin surface from FEM result

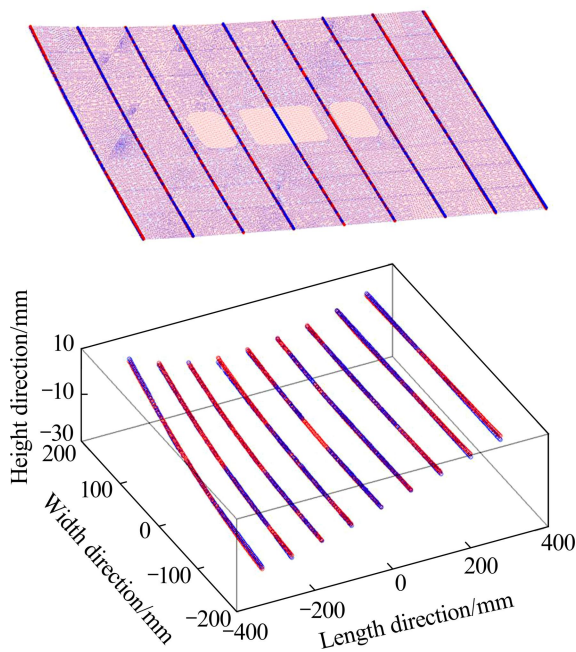


Fig. 11 Differences between formed outer skin surface and objective shape surface

5 Conclusions

1) An FEM model of press bend forming process of doubly curved integrally stiffened aircraft panel was established. A special simulation procedure and a new calculation method of the punch and die boundary conditions based on the bending line positions were proposed.

2) The Mises stress distributions at each bending step were analyzed. It was found that the influences among different bending steps are remarkable, and the deformation areas may overlap each other. Therefore, the panels experience cyclic loading and unloading conditions.

3) With quantitative comparisons, it can be concluded that the forming quality of the seven step press bend forming is quite good, considering both the

forming precision and the surface quality.

4) The simulation results show that this FEM model could well simulate the real fabrication process, so that it could assist in studying this complicated forming process. Establishment of the FEM model offers an efficient tool to understand press bend forming process, but it is just the beginning of the research. As the press bend forming path is the key factor that determines the final contour of the panel, an optimization method combined needs to be proposed to plan the best forming path. Hopefully this work will greatly help improving the dimensional accuracy and forming quality.

References

- [1] MUNROE J, WILKINS K, GRUBER M. Integral Airframe Structures (IAS)—Validated Feasibility Study of Integrally Stiffened Metallic Fuselage Panels for Reducing Manufacturing Costs [R]. NASA/CR-2000-209337, Seattle, Washington: Boeing Commercial Airplane Group, 2000: 1–6.
- [2] ZHAO G Y, LIU Y L, YANG H, LU C H, GU R J. Three-dimensional finite-elements modeling and simulation of rotary-draw bending process for thin-walled rectangular tube [J]. Materials Science and Engineering A, 2009, 499(1–2): 257–261.
- [3] YANG He, GU Rui-jie, ZHAN Mei, LI Heng. Effect of frictions on cross section quality of thin-walled tube NC bending [J]. Transactions of Nonferrous Metals Society of China, 2006, 16(4): 878–886.
- [4] BAI Qian, YANG He, ZHAN Mei. Finite element modeling of power spinning of thin-walled shell with hoop inner rib [J]. Transactions of Nonferrous Metals Society of China, 2008, 18(1): 6–13.
- [5] LIU Jin-song, ZHANG Shi-hong, WANG Zhong-tang. Experiment and simulation on the incremental bend forming technology of the integral wing-skin panel [J]. Metal Forming Technology, 2003, 21(6): 23–25. (in Chinese)
- [6] LIU Jin-song, ZHANG Shi-hong, ZENG Yuan-song, LI Zhi-qiang, REN Li-mei. Simulation of incremental forming of integral panel skin with grid-type ribs [J]. Materials Science and Process, 2004, 12(5): 515–517. (in Chinese).
- [7] LIU Jin-song, XU Yi, ZHANG Shi-hong, ZENG Yuan-song, WU Wei, ZHANG Xin-hua, WANG Zhong-tang, REN Li-mei. Finite element simulation of stress and strain on the incremental bend forming technology of the integral wing-skin panel [J]. Journal of Plasticity Engineering, 2003, 10(5): 42–45. (in Chinese).
- [8] REN Li-mei, WANG Zhong-tang, LIU Jin-song, ZHANG Shi-hong. Analysis and numerical simulation on stability in irregular section of ribs bending process [J]. Journal of Plasticity Engineering, 2003, 10(5): 39–41. (in Chinese)
- [9] LIU Jin-song. Incremental forming and self-adapting control on integral panel skin with grid-type ribs [D]. Shenyang: Institute of Metal, Chinese Academy of Science, 2004: 1–14. (in Chinese)
- [10] JIANG Nian-xiang, LIU Jin-song, ZENG Yuan-song. Research on the parameter forecasting of self-adapting incremental bending forming on integral panel skin with grid-type ribs [J]. Transactions of Shenyang Ligong University, 2006, 25(3): 15–18. (in Chinese)
- [11] LIU Jin-song, ZHANG Shi-hong, ZENG Yuan-song, LI Zhi-qiang, WANG Zhong-tang, XU Yi. Determination of feature line equation for self-adapting incremental press bending [J]. Journal of Materials Science and Technology, 2004, 20(6): 739–742.
- [12] YUE Feng-li, LIU Jin-song, ZHANG Shi-hong, ZENG Yuan-song.

- Knowledge base research on the incremental press bending technology of integral wing-skin panel [J]. Materials Science and Technology, 2008, 16(3): 306–309. (in Chinese)
- [13] MERCER C D, NAGTEGAAL J D, REBELO N. Effective application of different solvers to forming simulations [C]// Ithaca Proceedings of NUMIFORM'95. Ithaca, New York: NUMIFORM'95, 1995: 469–474.
- [14] YAN Yu, WAN Min, WANG Hai-bo. Prediction of fracture in press bend forming of aluminum alloy high-stiffener integral panels [J]. Computational Materials Science, 2011, 50(7): 2232–2244.
- [15] YAN Yu, WAN Min, WANG Hai-bo. Prediction of the stiffener buckling in the press bend forming of the integral panel [J]. Transactions of Nonferrous Metals Society of China, 2011, 21(11): 2459–2465.
- [16] YAN Yu, WAN Min, WANG Hai-bo, HUANG Lin. Optimization for the press bend forming path of aircraft integral panel [J]. Transactions of Nonferrous Metals Society of China, 2010, 20(2): 294–301.
- [17] YAN Yu, WAN Min, WANG Hai-bo. FEM equivalent model for press bend forming of aircraft integral panel [J]. Transactions of Nonferrous Metals Society of China, 2009, 19(2): 414–424.
- [18] WAGONER R H, LIB M. Simulation of springback: Through-thickness integration[J]. International Journal of Plasticity, 2007, 23: 345–360.

双曲率飞机整体壁板压弯成形有限元建模

阎 昱¹, 王海波¹, 万 敏²

1. 北方工业大学 机电工程学院, 北京 100144;
2. 北京航空航天大学 机械工程及自动化学院, 北京 100191

摘 要: 为了建立压弯成形工艺的有限元模型, 提出一种特殊的模拟过程和一种基于压弯线坐标的上下模边界条件计算方法。实现了双曲率飞机整体壁板七道次压弯成形工艺的模拟并且可以较好地模拟真实的生产过程, 本建模方法可用于此复杂成形工艺的研究。分析了应力和应变分布, 揭示了成形工艺的变形机理。通过进行定量的比较, 得知七道次压弯成形的成形精度和表面质量较好。

关键词: 压弯成形; 飞机整体壁板; 双曲率外形; 有限元建模

(Edited by YANG You-ping)